Native Cone Photoreceptor Cyclic Nucleotide-Gated Channel Is A Heterotetrameric Complex Comprising both CNGA3 and CNGB3: A Study Using the Cone-Dominant Retina of Nrl⁻/⁻ Mice

Alexander V. Matveev, **Alexander B. Quiambao**, **J. Browning Fitzgerald**, and **Xi-Qin Ding**
The Department of Cell Biology, University of Oklahoma Health Sciences Center, Oklahoma City, Oklahoma 73104, USA

Abstract

Cone vision mediated by photoreceptor cyclic nucleotide-gated (CNG) channel activation is essential for central and color vision and visual acuity. Mutations in genes encoding the cone CNG channel subunits, CNGA3 and CNGB3, have been linked to various forms of achromatopsia and progressive cone dystrophy in humans. This study investigates the biochemical components of native cone CNG channels, using the cone-dominant retina in mice deficient in the transcription factor neural retina leucine zipper (Nrl). Abundant expression of CNGA3 and CNGB3 but no rod CNG channel expression was detected in Nrl$^{-/-}$ retina by Western blotting and immunolabeling. Localization of cone CNG channel in both blue (S)- and red/green (M)-cones was shown by double immunolabeling using antibodies against the channel subunits and against the S- and M-opsins. Immunolabeling also showed co-localization of CNGA3 and CNGB3 in the mouse retina. Co-immunoprecipitation demonstrated the direct interaction between CNGA3 and CNGB3. Chemical cross-linking readily generated products at sizes consistent with oligomers of the channel complexes ranging from dimeric to tetrameric complexes, in a concentration- and time-dependent pattern. Thus this work provides the first biochemical evidence showing the inter-subunit interaction between CNGA3 and CNGB3 and the presence of heterotetrameric complexes of the native cone CNG channel in retina. No association between CNGA3 and the cone Na^+/Ca^{2+}-K^+ exchanger (NCKX2) was shown by co-immunoprecipitation and chemical cross-linking. This may implicate a distinct modulatory mechanism for Ca^{2+} homeostasis in cones compared to rods.

Keywords

Photoreceptor cyclic nucleotide-gated (CNG) channels are fundamental to phototransduction. In the dark, rod channels are activated by the binding of cGMP, allowing a steady cation current of Ca^{2+} and Na^+ to flow into the outer segment. Light triggers a sequence of enzymatic reactions that leads to the hydrolysis of cGMP. When CNG channels close, the inward current ceases and the cell hyperpolarizes (Pugh EN Jr 2000, Kaupp *et al.* 1989). An analogous phototransduction scheme is thought to exist in cones. However, the cGMP sensitivity, Ca^{2+} permeation, and functional modulation are profoundly different between the cone and rod CNG channels (Picones & Korenbrot 1995b, Rebrik & Korenbrot 1998).

Address correspondence and reprint requests to: Dr. Xi-Qin Ding, Department of Cell Biology, University of Oklahoma Health Sciences Center, 940 Stanton L. Young Blvd., BMSB 553, Oklahoma City, Oklahoma 73104, USA. E-mail: xi-qin-ding@ouhsc.edu.

Rod and cone CNG channels comprise two structurally related subunit types, CNGA1 and CNGB1 for the rod channel and CNGA3 and CNGB3 for the cone channel. For both rod and cone CNG channels, the A subunits are the primary subunits while the B subunits function in a modulatory role (Kaupp & Seifert 2002). Proper inter-subunit interaction, complex assembly and plasma membrane targeting have been shown to be vital for the channel function (Gordon *et al.* 1997, Kaupp & Seifert 2002, Huttl *et al.* 2005, Faillace *et al.* 2004).

Compared to the more advanced understanding of rod CNG channel structure and function (Kaupp & Seifert 2002, Weitz *et al.* 2002, Zhong *et al.* 2002), our knowledge of the native cone CNG channel is very limited. This is primarily due to the difficulty of investigating the cone system in a rod-dominant mammalian retina, as cones comprise only 3–5% of the total photoreceptor population. Although *CNGA3* gene has been cloned in human, bovine, mouse, rat, chicken, and striped bass (Wissinger *et al.* 1997, Hirano *et al.* 2000, Biel *et al.* 1994, Misaka *et al.* 1997, Bonigk *et al.* 1993, Weyand *et al.* 1994) and *CNGB3* gene has been cloned in human, canine, mouse, and striped bass (Gerstner *et al.* 2000, Sidjanin *et al.* 2002, Paillart *et al.* 2006, Kohl *et al.* 2000), the biochemical components of native cone CNG channel have never been determined. Studies using heterologous expression system (Peng *et al.* 2003, Peng *et al.* 2004) and isolated cones from retinas of striped bass (Rebrik & Korenbrot 2004, Rebrik *et al.* 2000) have added significantly to our understanding of the functional properties of cone CNG channel and its modulation. However, the nature of heteromeric complex of native cone CNG channel remains to be established.

Nevertheless, naturally occurring mutations in cone CNG channel subunits have been linked to a variety of inherited human cone diseases, including various forms of achromatopsia and progressive cone dystrophy (Kohl *et al.* 2000, Kohl *et al.* 1998, Wissinger *et al.* 2001). In fact, mutations in *CNGA3* and *CNGB3* genes account for nearly 70% of patients with achromatopsia, early-onset macular degeneration (under age 50), and other hereditary cone diseases (Nishiguchi *et al.* 2005). Over 50 mutations have been identified in human *CNGA3* gene (Wissinger et al. 2001). A number of studies have been carried out to identify the functional consequences of the disease-associated mutations in human CNGA3 and CNGB3 (Faillace et al. 2004, Patel *et al.* 2005, Liu & Varnum 2005). Mice with CNGA3 deficiency display loss of cone function and cone photoreceptors (Biel *et al.* 1999).

The cone-dominant retina in mice deficient in the transcription factor neural retina leucine zipper (Nrl) (Mears *et al.* 2001) has afforded a promising model to study cone specific proteins. The protein Nrl is a basic-motif leucine zipper transcription factor that is preferentially expressed in rod photoreceptors and is essential for the normal development of rods. Mice lacking the *Nrl* gene have no rods, but have increased numbers of S-cones, manifested as the loss of rod function and elevated cone function (Mears et al. 2001). Nrl$^{-/-}$ retinas display cone-like nuclear morphology, short and disorganized outer segments with rosette-like structure, apparent functional transformation of rods into cones, and the characteristics of cone gene expression profiles (Mears et al. 2001, Yu *et al.* 2004). Electrophysiological studies on isolated single photoreceptor cells from Nrl$^{-/-}$ retina demonstrated expression of functional S- and M-cone opsins in these cells (Nikonov *et al.* 2005). These mice have been used as a cone model in a variety of studies of cone specific proteins and cone phototransduction (Dang *et al.* 2004, Raven *et al.* 2007, Wenzel *et al.* 2007, Zhu *et al.* 2003, Farjo *et al.* 2006).

This study determined the biochemical components of native cone CNG channel using Nrl$^{-/-}$ retinas. The robust expression of the cone CNG channel and the absence of expression of the rod CNG channel were shown in Nrl$^{-/-}$ retinas, demonstrating its suitability as a model to study cone CNG channel in mammals. We demonstrated for the first time the direct interaction between CNGA3 and CNGB3 and the presence of heterotetrameric complexes of the native cone CNG channel in retina.

MATERIALS AND METHODS

Animals, antibodies and other materials

$Nrl^{-/-}$ mice were kindly provided by Dr. Anand Swaroop (University of Michigan). Wild-type mice (C57BL/6J background) were purchased from Charles River Laboratories (Wilmington, MA). All experiments and animal maintenance were approved by the local Institutional Animal Care and Use Committee (Oklahoma City, Oklahoma) and conformed to the guidelines on the care and use of animals adopted by the Society for Neuroscience and the Association for Research in Vision and Ophthalmology (Rockville, Maryland).

Rabbit polyclonal antibodies against peptides corresponding to the sequence between residues 77 and 97 (SNAQPNPGEQKPPDGGEGRKE) of mouse CNGA3 and regions between 476 and 489 (CEYTWNSQRILDESN) and between 677 and 694 (CKVDLGRLLKGKRKTTTQK) of mouse CNGB3 were generated and used in this study. The rat monoclonal antibody CNC-7D8 was kindly provided by Dr. Benjamin Kaupp (The Institute of Neurosciences and Biophysics, Forschungszentrum, Jülich, Germany). Monoclonal antibodies against bovine CNGA1 (PMc 1D1), glutamic acid-rich protein (GARP), and rhodopsin were kindly provided by Dr. Robert Molday (University of British Columbia, Vancouver, Canada). Rabbit polyclonal antibodies against mouse blue (S)- and red/green (M)-opsins were kindly provided by Dr. Muna Naash (University of Oklahoma Health Sciences Center, Oklahoma). Rabbit polyclonal antibody against the cone Na^+/Ca^{2+}-K^+ exchanger (NCKX2) was kindly provided by Dr. Jonathan Lytton (University of Calgary Health Sciences Centre, Calgary, Canada). Goat polyclonal anti-S-cone opsin antibody was purchased from Santa Cruz Biotechnology, Inc. (Santa Cruz, CA). Monoclonal anti-actin antibody was purchased from Abcam, Inc. (Cambridge, MA). Secondary, horseradish peroxidase (HRP)-conjugated anti-rabbit or anti-mouse antibodies were purchased from Kirkegaard & Perry Laboratories Inc. (Gaithersburg, MD). Human CNGB3 cDNA was kindly provided by Dr. Hisao Ueyama (The Shiga University of Medical Science, Seta, Japan). Chemical cross-linkers BMDB (1,4-bismaleimidyl-2,3-dihydroxybutane) and BS^3 (bis-sulfosuccinimidyl suberate) were purchased from Pierce (Rockford, IL). Calmodulin (CaM) affinity resin and 8-pCPT-cGMP were purchased from Sigma-Aldrich (St. Louis, MO). All other chemicals were purchased from Sigma-Aldrich (St. Louis, MO), Bio-Rad (Hercules, CA) or Invitrogen (Carlsbad, CA).

Retinal membrane preparation and detergent solubilization

Retinas were homogenized in homogenization buffer [10 mM Tris-HCl, pH 7.4, 1 mM EDTA, 200 mM sucrose, 1 mM phenylmethylsulfonyl fluoride (PMSF)]. The nuclei and cell debris were removed from the homogenate by centrifugation at $1000 \times g$ for 5 min at 4°C. The resulting supernatant was centrifuged at $16,000 \times g$ for 30 min at 4°C. The resultant membranes were used in chemical cross-linking experiments or solubilized in solubilization buffer (50 mM Tris–HCl, pH 7.5, 100 mM NaCl, 5 mM EDTA, 0.05% SDS, 2.5% glycerol and 1.0 mM PMSF) containing either 1% Triton X-100 or 60 mM octylglucoside (OG), or in CHAPS buffer (10 mM Hepes-KOH, pH 7.4, 1 mM DTT, 10 mM $CaCl_2$, 0.15 M KCl, 18 mM CHAPS, and 1.0 mM PMSF) at 4°C for 4 h. The protein (membrane):detergent ratios for Triton X-100, OG, and CHAPS were 1:3.3, 1:5.8 and 1:3.6, respectively. The supernatants were separated by centrifugation at $100,000 \times g$ for 60 min at 4°C. The solubilized membrane proteins were used in immunoprecipitation and CaM affinity binding assays. Protein concentration was assessed using a Bio-Rad Protein Assay kit (Bio-Rad Laboratories, Hercules, CA).

SDS-PAGE and Western blot analysis

The protein samples (membrane or soluble proteins, 30 µg) were subjected to SDS-PAGE and transferred onto polyvinylidene diflouride (PVDF) membranes. Following overnight blocking

in 5% milk at 4°C, blots were incubated with primary antibodies at appropriate dilution ratios (CNGA3 and CNGB3, 1:250; GARP, 1:50; NCKX2, 1:250; actin, 1:5000) for 2 h at room temperature. After 3×10 min washings with Tris-buffered saline with 0.1% Tween 20 (TBST), the blots were incubated with HRP-conjugated secondary antibodies (1:12,500) for 1 h at room temperature. SuperSignal® West Dura Extended Duration chemiluminescent substrate (Pierce, Rockford, IL) was used to detect binding of the primary antibodies to their cognate antigens and images were captured using a Kodak Imaging Station (4000 R).

Retinal section preparation, immunofluorescence labeling, and confocal microscopy

Mouse eyes were enucleated and fixed with 4% formaldehyde (Polysciences, Inc., Warrington, PA) in 0.1 M sodium phosphate buffer, pH 7.4 for 16 h at 4°C. When necessary, the superior portion of the cornea was marked for orientation prior to enucleation. Fixed eyes were then transferred to PBS or 0.1 M sodium phosphate buffer, pH 7.4, containing 0.02% sodium azide, for storage until processing. Paraffin or cryo-embedding were performed based on the antibody labeling efficiency and specificity (see Supplementary Table 1). Sections were prepared using a Leica microtome (for the paraffin-sections, 5 µm) and Leica cryostat (for the cryo-sections, 14 µm), respectively.

Immunofluorescence labelings were performed as described previously (Ding *et al.* 2004, Stricker *et al.* 2005). Briefly, eye sections were blocked with PBS containing 5% BSA and 0.5% Triton-X 100 for 1 h at room temperature. When necessary, antigen retrieval was performed (see the Supplementary Table 1) by incubating tissues in 0.01M sodium citrate buffer, pH 6.0, for 30 minutes in a 65°C water bath before blocking. Primary antibody incubation [CNGA3 (rabbit polyclonal), 1:250; CNGA3 (CNC-7D8, rat monoclonal), 1:50; CNGB3, 1:250; S-opsin, 1:500; M-opsin, 1:500; CNGA1 (PMc 1D1), 1:50; GARP (4B1), 1:50; NCKX2 (Fab), 1:100] was performed at room temperature for 2 h. Following Alexa-conjugated secondary antibody incubation (at room temperature for 30 min) and rinses, slides were mounted and cover-slipped. The fluorescent signals were visualized and images were captured using an Olympus AX70 fluorescence microscope (Olympus Corp., Center Valley, PA) with the QCapture imaging software (QImaging Corp., Surrey, BC, Canada) and an Olympus IX81-FV500 confocal laser scanning microscope (Olympus, Melville, NY) with the FluoView imaging software (Olympus).

Reverse transcription-polymerase chain reaction (RT-PCR)

RT-PCR was carried out on total retinal RNA using an oligo-dT primer and Superscript II reverse transcriptase (Invitrogen, Carlsbad, CA). Amplification of the mouse CNGA1 (NCBI Accession #: NM_007723) full length coding region was performed using the forward primer 5'-GTCTCATTTAAACAAGCGCAG -3' and the reverse primer 5'-GTTTGGCTGTTGACCAGCTT -3'. The neuronal housekeeping gene hypoxanthine phosphoribosyltransferase (HPRT) was included as an internal control.

Immunoprecipitation and CaM binding

Anti-CNGA3 affinity column was prepared and used for immunoprecipitation. The polyclonal antiserum was purified via Protein A Sepharose beads (Kirkegaard & Perry Laboratories, Inc., Gaithersburg, MD) and the purified antibody was covalently cross-linked onto the CNBr-activated Sepharose resin (GE Healthcare, Uppsala, Sweden) to generate the antibody affinity resin. CHAPS-solubilized membrane proteins (200 µg) were incubated with the antibody affinity resin (100 µl) in solubilization buffer at 4°C overnight. For immunoprecipitation using anti-NCKX2 antibody, solubilized membrane proteins were incubated with the antibody (dilution ratio of 1:100) in the CHAPS solubilization buffer overnight at 4°C. Protein A Sepharose beads were then added and incubation continued at 4°C for another 1 h. After adsorption, the beads were washed with solubilization buffer three times (500 µl for each wash),

and bound proteins were eluted with Laemmli sample buffer, followed by gel electrophoresis and immunoblotting.

CaM binding to cone CNG channel was examined using CaM affinity resin as described by Molday et al. (Molday & Molday 1999). Briefly, the CHAPS-solubilized retinal membrane proteins (200 µg) were incubated with the affinity resin (50 µl) in CHAPS binding buffer [10 mM Hepes-KOH, pH 7.4, 1 mM dithiothreitol (DTT), 1.0 mM $CaCl_2$, 0.15 M KCl, 18 mM CHAPS, 0.2% asolectin and protease inhibitor mixture] in the presence and absence of 5.0 mM EDTA at 4°C for 2 h. The resin was washed three times with the same buffer and bound proteins were eluted with Laemmli sample buffer and resolved by 10% SDS-PAGE, followed by Western blot analysis.

Chemical cross-linking

These experiments were performed as described by Weitz et al. (Weitz et al. 2002) using membrane preparations from $Nrl^{-/-}$ retinas. The thiol-specific cross-linker BMDB and the amino-specific cross-linker BS^3 were used as bio-functional cross-linkers. In thiol-specific cross-linking, two sequential pre-treatments on the membranes were performed. To block all accessible thiol groups, the membranes were first incubated with N-ethylmaleimide (NEM) (Sigma-Aldrich, St. Louis, MO) in Hepes buffer (10 mM Hepes, pH 7.4, 100 mM NaCl) at room temperature for 10 min, followed by wash with the same buffer without NEM. Membranes were then incubated with 50 µM 8-pCPT-cGMP at room temperature for 10 min to activate the channel (opening of the channel) before addition of the cross-linker BMDB. The concentration-dependent reactions were performed using 0.05, 0.2, 0.4 mM BMDB at room temperature for 20 h. The cross-linking reactions were terminated by addition of 5.0 mM DTT. The time-dependent reactions were performed using 0.2 mM BMDB and the reactions were terminated at 1, 3, 5, 7, 20 h. In amino-specific cross-linking, membranes were incubated with 0.3, 0.5, and 1.0 mM of BS^3 at room temperature for 30 min. The time-dependent reactions were performed using 0.5 mM BS^3 and the reactions were terminated at 2, 5, 10, 30 min. The cross-linking reaction was terminated by addition of 500 mM Tris-HCl (pH 7.5). BS^3 acts fast but can be hydrolyzed quickly in solution. Therefore the duration of the cross-linking reaction is short. BMDB, on the other hand, is quite stable in solution and is usually used for longer duration (Weitz et al. 2002). Cross-linked products were resolved by 3–8% Nu-PAGE (Invitrogen, Carlsbad, CA) and analyzed by Western blotting.

Cell culture and transfection

Human embryonic kidney (HEK) 293 cells were routinely cultured in Dulbecco's modified Eagle's medium (DMEM) supplemented with 10% fetal bovine serum and 1% penicillin/ streptomycin at 37°C in a humidified atmosphere with 5% CO_2. Cells were transfected at 70 to 80% confluence with cDNAs for mouse CNGA3 (Ding *et al.* 2008) or human CNGB3 (Okada *et al.* 2004) by calcium phosphate method and used for experiments ~48 h post-transfection.

RESULTS

Expression and cellular localization of cone CNG channel in the mouse retina

Using the antibodies against the channel subunits, abundant amounts of CNGA3 and CNGB3 were detected in $Nrl^{-/-}$ retinas by Western blotting and immunolabeling. Retinal membrane preparations were used for Western blot analysis. A single band with migration corresponding to M_r ~73 kDa, equivalent to the predicted size (72.2 kDa) of CNGA3, was detected by the polyclonal anti-CNGA3 antibody (Figure 1A, upper panel). Similarly, a dominant band migrating at M_r ~76 kDa, consistent with CNGB3, was detected by the CNGB3 antibody, similar to its predicted size (79.7 kDa) (Figure 1A, middle panel). The anti-CNGA3 antibody

has been used to detect the endogenous channel subunit in the mouse retina and the channel subunit heterologously expressed in HEK 293 cells (Ding et al. 2008). The specificity of the anti-CNGA3 and anti-CNGB3 was shown by the peptide competition experiments (see Supplementary Figure 1 A–B). Amounts of CNGA3 and CNGB3 detected in $Nrl^{-/-}$ retina were significantly higher than those in the wild-type retina (normalized to actin as an internal control), which is consistent with the cone-dominant feature in this mouse model. Of note, the intensity ratio of the wild type to $Nrl^{-/-}$ retina for CNGB3 was higher than that for CNGA3. This may reflect a difference in the antibody detection abilities. The linear dynamic range for CNGB3 detection might be smaller than that of CNGA3, which could contribute to the observation.

Retinal expression and cone localization of CNGA3 and CNGB3 in the wild-type and $Nrl^{-/-}$ retinas were also shown by immunolabeling (Figure 1B–D). Using the rat monoclonal anti-CNGA3 antibody CNC-7D8 and the rabbit polyclonal anti-CNGB3, the cone punctuate staining was shown in the basal part of the outer segments of the wild-type retina (Figure 1B left panels and Figure 1D left upper panel) and ample immunoreactivity was detected in the rosette-like structures and in the cone outer segments of $Nrl^{-/-}$ retinal sections (Figure 1C left panels and 1D left lower panel). CNC-7D8 was generated in Dr. Benjamin Kaupp's laboratory and has been shown previously to label CNGA3 in the sections of rat retina and olfactory sensory neurons (Meyer *et al.* 2000). Specificity of the polyclonal anti-CNGB3 was demonstrated by the peptide pre-adsorption experiments (see Supplementary Figure 1 C–D). The disorganized outer segments with rosette-like structure were apparent in $Nrl^{-/-}$ retina as described previously in this mouse model (Mears et al. 2001, Farjo et al. 2006). Thus, using both immunoblotting and immunolabeling, an abundance of CNGA3 and CNGB3 was detected in the $Nrl^{-/-}$ retina. This study provides the first demonstration of expression of CNGB3 protein in the retina, since the genes encoding CNGB3 were cloned.

Cone localization of CNGA3 and CNGB3 in the wild-type and $Nrl^{-/-}$ retinas was examined by co-immunolabeling with antibodies against cone opsins. As shown in Figure 1B and 1C, localization of CNGA3 in S-cones and in M-cones in wild-type (Figure 1B) and $Nrl^{-/-}$ (Figure 1C) retinas was demonstrated by co-immunolabeling using CNC-7D8 with the rabbit polyclonal antibodies against S- or M-opsins. The double labeling shows that CNGA3 overlaps close to 100% with both S- and M-opsins. This observation is consistent with the finding that the most cones of mouse retina co-express both S- and M-opsins as described by Applebury et al. (Applebury *et al.* 2000). They showed that the levels of S-opsin are constant in all cones while the levels of M-opsin are graded from dorsal to ventral (Applebury et al. 2000). We did observe a less abundant co-labeling of CNGA3 with M-opsin in the $Nrl^{-/-}$ retina (Figure 1C, lower panels), which may reflect a region close to ventral where cones have less abundance of M-opsin. Functional co-expression of both cone pigments in a single mouse cone has also been demonstrated by suction pipetting recordings using $Nrl^{-/-}$ retinal slice (Nikonov et al. 2005). Figure 1D shows localization of CNGB3 in S-cones in wild-type (upper panels) and $Nrl^{-/-}$ (lower panels) retina by co-immunolabeling using the rabbit polyclonal anti-CNGB3 and the goat polyclonal anti-S-cone opsin. Images of high magnification are shown to the right of the merge images for a better visualization of the co-localization.

Lack of rod CNG channel expression in $Nrl^{-/-}$ retina

Comparative analysis of rod CNG channel expression in the $Nrl^{-/-}$ and wild-type retinas was performed by Western blotting, immunolabeling using antibodies against GARP (recognizing GARP part of CNGB1) and CNGA1, and by RT-PCR detection of CNGA1 mRNA. Figure 2A shows expression of CNGB1 (250 kDa band) and GARP (72 kDa band) in the wild-type retina; in contrast, no detection of these proteins in $Nrl^{-/-}$ retinas was evident. RT-PCR was performed to detect CNGA1 mRNA expression in wild-type and $Nrl^{-/-}$ retina, using primers

amplifying the full-length coding region of mouse CNGA1. As shown in Figure 2B, a 2.1 kb fragment was detected in wild-type retina, but not in Nrl$^{-/-}$ retina. Retinal expression and localization of rod CNG channel in wild-type, but not in Nrl$^{-/-}$ retinas were also demonstrated by immunostaining. Figure 2C shows immunolabeling of CNGA1 (left panels), GARP (middle panels), and rhodopsin (right panels) in wild-type retinal sections. The labeling of CNGA1 was achieved by using the cryo-sections (fixation time: 15 min). The short-time fixation may contribute to the rough morphological appearance of the retinal sections (Figure 2C, upper left pane). No immunolabeling was detected in Nrl$^{-/-}$ retinas with the same antibodies. Hence, these experimental results clearly show expression of cone CNG channel and lack of expression of rod CNG channel expression in the Nrl$^{-/-}$ retina, demonstrating its utility for studies of the cone CNG channel.

Expression and cellular localization of NCKX2 in the mouse retina

Association of the rod CNG channel with the rod Na^+/Ca^{2+}-K^+ exchanger (NCKX1) and its implications in local Ca^{2+}-signaling has been well documented (Kim *et al.* 1998, Bauer & Drechsler 1992, Bauer 2002). We decided to examine whether there is an association between the cone exchanger and the cone CNG channel. To do this, retinal expression and localization of NCKX2 were examined in Nrl$^{-/-}$ retinas by Western blotting and immunolabeling using the polyclonal antibody against NCKX2 (Li *et al.* 2006). As shown in Figure 3A, an ample amount of NCKX2 was detected in Nrl$^{-/-}$ retinas compared to the level in wild-type retina. Note that the antibody detected a pair of doublet bands. Both bands have been shown being specific to NCKX2 antibodies and are absent in NCKX2$^{-/-}$ mice (Li et al. 2006). It is believed that the differently sized bands are probably the products of alternatively spliced transcripts. One has been described previously (Tsoi *et al.* 1998) and one was newly identified in mouse (Li et al. 2006). Cone localization of NCKX2 in Nrl$^{-/-}$ retinas was shown by co-immunolabeling with antibodies against the exchanger and against S-opsin (Figure 3B).

Solubility of cone CNG channel to detergent extraction

Effective solubilization of channel complexes from membranes is critical for the subsequent biochemical analysis. Thus, we examined the solubility of CNGA3 and CNGB3 in different detergent extractions. The detergents used were Triton X-100 (1%), octyl glucoside (OG) (60 mM), and CHAPS (18 mM) and the membrane protein:detergent ratios were 1:3.3, 1:5.8 and 1:3.6, respectively. After solubilization, aliquots of supernatants and pellets (30 µg protein) were resolved by 10% SDS-PAGE, followed by Western blotting. Figure 4 shows representative images of Western blot detection of CNGA3 and CNGB3 following the membrane detergent solubilization. None of the detergents at the conditions used yielded a complete solubilization of the channel complexes. The channel remained in abundance in pellets and aggregated on the top of the gel following the detergent extraction. Compared to the two non-ionic detergents, the zwitterionic detergent CHAPS yielded a more favorable solubilization of the channel complex into its constituent subunits. In studies of rod CNG channel, CHAPS has been shown to be effective in solubilizing the channel complexes. The present results demonstrate comparable solubilization characteristics of the cone CNG channel. With the three types of detergents used, there were significant amounts of residual CNG channel protein remaining in the pellets, suggesting that a portion of the overall channel population resides in detergent-insoluble membrane domains.

Interaction between CNGA3 and CNGB3 in the mouse retina

While inter-subunit interaction and stoichiometry of the native rod CNG channel have been well studied, biochemical components of the native cone CNG channel has never been studied. This work examined the interaction between CNGA3 and CNGB3 in the mouse retina via co-immunoprecipitation. The CHAPS-solubilized membrane proteins prepared from Nrl$^{-/-}$

retinas were used in the immunoprecipitation assays. The resulting immunoprecipitates were resolved by 10% SDS-PAGE followed by immunoblotting. Figure 5A shows co-precipitation of CNGB3 in immunoprecipitation assays using the anti-CNGA3 antibody (upper and middle panels). These results were confirmed by immunoprecipitation using the anti-CNGB3 antibody. In these assays, both CNGB3 and CNGA3 were detected in the immunoprecipitation products (data not shown).

We also examined the potential interaction between CNGA3 and NCKX2. As shown in Figure 5A, no NCKX2 signal was detected in the CNGA3 immunoprecipitation assays (lower panel). Immunoprecipitation with the polyclonal anti-NCKX2 antibody were performed (Figure 5B). NCKX2 (both bands) was precipitated by the polyclonal anti-NCKX2 antibody (upper panel) but no signal of CNGA3 or CNGB3 was detected in the immunoprecipitation products (middle and lower panels). Hence, this study provided the first biochemical evidence showing the direct interaction between CNGA3 and CNGB3 in retina, demonstrating the presence of heteromeric channel complexes *in vivo*. Co-immunoprecipitation with antibodies against CNGA3 or against NCKX2 did not show evidence of interaction between the cone channel and the exchanger.

Oligomeric complexes of cone CNG channel in the mouse retina

Chemical cross-linking is a useful approach to study protein-protein interaction and the spatial proximity between two or more macromolecules. It has been successfully used to characterize rod CNG channel composition and stoichiometry. Thus, we performed chemical cross-linking to explore the nature of the cone CNG channel complex. Both thiol- (BMDB) and amino-specific (BS^3) cross-linkers were used in the cross-linking reactions with membranes prepared from $Nrl^{-/-}$ retinas. These two types of cross-linkers have been commonly used in studies of protein-protein interactions including characterization of the rod channel complexes and association between rod CNG channel and rod exchanger NCKX1 (Weitz et al. 2002, Schwarzer *et al.* 2000). The cross-linked products were separated by 3–8% NuPAGE and analyzed by Western blot analysis. Figure 6A shows a typical gel separation of the cross-linked products with varying concentrations of BMDB or BS^3, detected by antibodies against CNGA3, CNGB3 and NCKX2. The cross-linked products equivalent to the dimer (~150 kDa), trimer (~240 kDa), and tetramer (~320 kDa) of the channel, respectively, were detected by both anti-CNGA3 (Figure 6A, left panel) and anti-CNGB3 antibodies (Figure 6A, middle panel). Time courses of the cross-linking reaction were also performed using BS^3 (Figure 6B, upper panels) and BMDB (Figure 6B, lower panels). Channel complexes at sizes equivalent to the tetramer, trimer and dimer were detected in a time-dependent pattern. Thus, this work provided the first biochemical evidence showing the presence of tetrameric complexes of the cone CNG channel in retina. The potential association of cone CNG channel with NCKX2 was also examined with these cross-linking assays. The same blots were probed with the polyclonal anti-NCKX2 antibody. As shown in Figure 6A (right panel), no NCKX2-associated cross-linking products were detected in these experiments, which is consistent with findings obtained from co-immunoprecipitation assay (see Figure 5) and provides an additional evidence of lack of association between cone CNG channel and NCKX2.

Co-localization of CNGA3 and CNGB3 in the mouse retina

Co-localization of CNGA3 and CNGB3 in the mouse retina was examined by co-immunolabeling using the rat monoclonal anti-CNGA3 and the rabbit polyclonal anti-CNGB3. As shown in Figure 7, co-localization of CNGA3 and CNGB3 was demonstrated in retinal sections of the wild-type (Figure 7A) and $Nrl^{-/-}$ mice (Figure 7B). Images of high magnification are shown to the right of the merge images for a better visualization of the co-localization. These co-localization results provided additional supporting evidence showing the presence of heteromeric complex of cone CNG channel in the retina.

Binding of CaM to the cone CNG channel subunits in the mouse retina

CaM is known to be an important modulator for the olfactory and rod CNG channel. However, its role in the cone CNG channel remains disputed (Grunwald *et al.* 1999, Peng et al. 2003, Muller *et al.* 2001). We examined the potential modulatory role of CaM in cone CNG channel by examining its binding to cone CNG channel in the mouse retina. The CHAPS-solubilized membrane proteins prepared from mouse retinas were incubated with a CaM affinity resin in the presence or absence of 5.0 mM EDTA and bound proteins were resolved by 10% SDS-PAGE, followed by Western blot analysis for identity of the bound proteins. We observed a strong binding signal for CNGA3 and a very weak binding for CNGB3. Figure 8 shows that CNGA3 was readily detected as CaM-bound product but only a trace signal of CNGB3 binding was detected [note the signal detected in EDTA (+) sample]. Addition of EDTA abolished the binding, indicating a specific, Ca^{2+}-dependent binding.

DISCUSSION

In the last decade, a large number of mutations in genes encoding the cone CNG channel have been identified in patients with various forms of achromatopsia and/or progressive cone dystrophy (Kohl et al. 2000, Kohl et al. 1998, Sundin *et al.* 2000, Wissinger et al. 2001). This has stimulated a variety of studies on the cone CNG channel; from the channel biochemical characteristics (Zhong et al. 2002, Peng et al. 2004) and functional regulation (Muller et al. 2001, Peng et al. 2003) to molecular defects of the disease-causing mutations (Patel et al. 2005, Liu & Varnum 2005, Faillace et al. 2004). However, due to the low abundance of cones in mammalian retinas, biochemical studies of native cone CNG channel and the interacting proteins have been a long-standing challenge. Although retinas of diurnal mammals (such as ground squirrel or chipmunks), which have high population of cones, can be used as tools to study cone biochemistry and cone proteins, our limited genetic knowledge and limited ability to genetically manipulate these species has restricted use of these animals. Thus current knowledge of the cone CNG channel biochemistry is essentially all from studies in heterologous expression system. Little work has been documented using the native cone channel preparation from the time the genes for CNGA3 and CNGB3 were cloned (Wissinger et al. 1997, Gerstner et al. 2000, Bonigk et al. 1993, Hirano et al. 2000, Yu *et al.* 1996, Paillart et al. 2006, Weyand et al. 1994).

This work examined expression, biochemical composition, and protein interactions of the cone CNG channels using the cone-dominant retinas of $Nrl^{-/-}$ mice. Robust expression of cone CNG channel and lack of rod CNG channel expression were determined in $Nrl^{-/-}$ retina. Cone-localization of the channel subunits CNGA3 and CNGB3 in the mouse retina was demonstrated by co-immunolabeling using antibodies against the channel subunits and against the S- and M-cone opsins. Thus our results show that the $Nrl^{-/-}$ retina can serve as a useful tool to study native cone CNG channel in mammals. Retinas of $Nrl^{-/-}$ mice have no rods but have increased numbers of S-cones, manifested as the loss of rod function and elevated cone function, and show characteristics of cone gene expression profiles (Mears et al. 2001, Yu et al. 2004). Morphologically, $Nrl^{-/-}$ retinas display cone-like nuclear appearance and short and disorganized outer segments with rosette-like structure (Daniele *et al.* 2005, Mears et al. 2001). Electrophysiological studies on isolated single photoreceptor cells from $Nrl^{-/-}$ retina demonstrated expression of functional S- and M-cone opsins in these cells (Nikonov et al. 2005). Despite the abnormal morphological appearance, many morphological, molecular, and electrophysiological features of the $Nrl^{-/-}$ photoreceptors are cone-like and distinguish these cells from rods (Daniele et al. 2005). Indeed, this mouse line has been used as a cone model to study cone function and phototransduction and cone specific proteins (Dang et al. 2004, Raven et al. 2007, Wenzel et al. 2007, Zhu et al. 2003).

The biochemical components and stoichiometry of the rod CNG channel has been well characterized (Kaupp & Seifert 2002, Weitz et al. 2002, Zheng *et al.* 2002, Zhong et al. 2002). This is a result of two factors: 1) the large number of rod photoreceptors in most mammalian retinas, which facilitates the isolation of abundant CNG protein (*e.g.*, channel complexes purified from bovine retinas), and 2) the distinct molecular mass difference between the A and B subunits (CNGA1 *vs.* CNGB1: 62 kDa *vs.* 240 kDa), which provides an advantage in biochemical characterization of the channel complex stoichiometry. Studies have demonstrated that the rod CNG channel is a complex with a stoichiometry of three CNGA1 subunits and one CNGB1 subunit (Zheng et al. 2002, Weitz et al. 2002, Shammat & Gordon 1999). It is also well documented that the function and modulation of rod CNG channel relies on the proper subunit interaction and complex assembly (Gordon et al. 1997, Matulef & Zagotta 2002, Varnum & Zagotta 1997). The present work examined the biochemical components of the native cone CNG channel. We showed for the first time the co-localization of CNGA3 and CNGB3, the interaction between the two types of the subunits, and the presence of the tetrameric complexes in the mouse retina. These results demonstrate that the native cone CNG channel is a heterotetrameric complex comprising both CNGA3 and CNGB3. There have been two reports describing the stoichiometry of cone CNG channel. The report from Zhong et al using HEK 293 cells proposed a 3A:1B stoichiometry (Zhong et al. 2002), while a 2A:2B stoichiometry was proposed by Peng et al from their *Xenopus* oocytes work (Peng et al. 2004). Nrl$^{-/-}$ retina provide a unique resource to determine the stoichiometry of the native cone CNG channel.

CNG channel provides the only source for Ca^{2+} influx into the outer segments. Interaction of rod CNG channel (through CNGA1 subunit) with NCKX1 and functional significance of such association in control of the intracellular Ca^{2+} concentration and dynamics of Ca^{2+} homeostasis have been well characterized (Bauer & Schauf 2002, Schwarzer et al. 2000, Bauer 2002, Weitz et al. 2002). Little is known about the association between cone CNG channel and NCKX2. Hence we examined the potential interaction between CNGA3 and NCKX2. Cone specific expression of NCKX2 was detected in Nrl$^{-/-}$ retina but no evidence of such interaction was obtained as analyzed by co-immunoprecipitation assays. As a non-covalent association may be influenced by the nature of the detergent (and other conditions) used to solubilize the membrane, an existing association may not be detected in a given immunoprecipitation assay. Also if NCKX2 is preferentially associated with the CHAPS-insoluble portion of the channel, immunoprecipitation using the CHAPS-solubilized membrane proteins may not be able to detect the existing interaction. Thus a negative immunoprecipitation result may not necessarily indicate the absence of the interaction. We further examined the spatial approximation between the cone channel and the exchanger by chemical cross-linking using the retinal membrane preparations. Complexes of the cone CNG channel were detected in the cross-linking products but no NCKX2 at the oligomeric sizes was detected in the same assays (see Figure 6). Thus the co-immunoprecipitation results were supported by the observations of the chemical cross-linking. The observation of the lack of interaction between the cone CNG channel and the cone exchanger is in agreement with a recent report showing a normal retinal phenotype in NCKX2$^{-/-}$ mice (Li et al. 2006). Cone and rod function and retinal morphology in NCKX2$^{-/-}$ mice appeared indistinguishable from that of the wild-type animals (Li et al. 2006). Thus, NCKX2 may not be the major component required for Ca^{2+} extrusion in cones and a distinct modulatory mechanism of Ca^{2+} influx and efflux may exist. It has been shown that the relative Ca^{2+} permeability of CNG channels and the dark current carried by Ca^{2+} in cones were about two- to three-fold larger than that in rods (Picones & Korenbrot 1992, Picones & Korenbrot 1995a). Also, light-triggered changes in cytoplasmic free Ca^{2+} were much faster in outer segments of cones than rods (Paillart *et al.* 2007, Picones & Korenbrot 1992, Picones & Korenbrot 1995a). Thus it is worthy to explore the molecule(s) involved in the modulation of the Ca^{2+} homeostasis in cones. A study by Kang et al. indicated that the interaction between the CNG channels and the Na^+/Ca^{2+}-K^+ exchangers was not isoform-specific, *i.e.* the rod

exchanger could interact with the cone channel subunit, and *vice versa* (Kang *et al.* 2003). However, in a recent study by Paillart et al., NCKX1 was shown to be expressed in rods but not in cones (Paillart et al. 2007). Hence, it appears less likely that NCKX1 associates with cone CNG channel to modulate the Ca^{2+} homeostasis.

CNG channels do not desensitize in the continued presence of the ligand (Kaupp & Seifert 2002). Activity of the rod and olfactory channel appears to be modulated by the Ca^{2+}/CaM system (Balasubramanian *et al.* 1996, Trudeau & Zagotta 2002, Trudeau & Zagotta 2003, Weitz *et al.* 1998), by phosphorylation (Chae *et al.* 2007, Molokanova *et al.* 2000) and by phosphatidylinositol-3,4,5-trisphosphat (PIP$_3$) (Brady *et al.* 2006, Bright *et al.* 2007). However, modulation of cone CNG channel remains obscure and the role of CaM appears complicated. Cone CNG channels in excised patches from chick retina (Bonigk *et al.* 1996) and heteromeric channels in heterologous expression system (Peng et al, 2003) were shown to be modulated by CaM, while native cone CNG channels of fish (Haynes & Stotz 1997, Hackos & Korenbrot 1997) and homomeric channels in heterologous expression system were found to be insensitive to CaM (Grunwald et al. 1999, Yu et al. 1996, Muller et al. 2001). Of note, a Ca^{2+}-dependent modulation of cone CNG channel through an unknown soluble Ca^{2+}-binding protein other than CaM has been well described (Rebrik & Korenbrot 1998, Rebrik et al. 2000, Rebrik & Korenbrot 2004).

In its N-terminal region CNGA3 comprises a fairly conserved CaM target motif that showed CaM binding in various *in vitro* binding assays (Bonigk et al. 1996, Grunwald et al. 1999, Muller et al. 2001, Peng et al. 2003). The present work examined the binding of CaM to the native cone CNG channel complexes in the mouse retina. We confirmed binding of CaM to CNGA3 but only a trace binding to CNGB3 was observed. The latter does not support the finding by Peng et al. (Peng et al. 2003) in which CaM was shown to bind to CNGB3 in the gel overlay assays using the GST fusion proteins. The feeble signal observed in this study may reflect a weak binding to CNGB3 or may indicate an indirect detection through CNGA3. The uneven binding signals detected may also suggest a competitive interaction between CaM and CNGB3 existing on CNGA3. In this case, binding of CaM to CNGA3 replaces CNGB3. The competitive interaction with the channel subunit has been described in rod CNG channel (Trudeau & Zagotta 2002). Binding of CaM to CNGB1 was shown to disrupt the interaction between CNGB1 and CNGA1, which leads to inhibition of channel activity (Trudeau & Zagotta 2002). Thus if there is a competitive binding among the three elements, the binding partner of CaM to the cone channel is different from that in rod channel. CaM primarily binds to the B subunit (CNGB1) of the rod channel but it appears to bind primarily to the A subunit (CNGA3) of the cone channel. Hence, if cone CNG channel is modulated by CaM, the mechanism behind this may be different from that in the rod channel.

This study demonstrates the value of the Nrl$^{-/-}$ retina as a tool for studying the native cone CNG channel in mammals and provides the first biochemical evidence showing the interaction between CNGA3 and CNGB3 and the presence of heterotetrameric complexes of the native cone CNG channel in retina. No association between CNGA3 and NCKX2 was shown by co-immunoprecipitation and chemical cross-linking. This may indicate a distinct modulatory mechanism for Ca^{2+} homeostasis in cones compared to rods.

Supplementary Material

Refer to Web version on PubMed Central for supplementary material.

Footnotes

CNG, cyclic nucleotide-gated

cGMP, cyclic guanosine monophosphate
NCKX2, cone Na^+/Ca^{2+}-K^+ exchanger
Nrl, neural retina leucine zipper
PBS, phosphate-buffered saline
GARP, glutamic acid-rich protein
PMSF, phenylmethylsulfonyl fluoride
OG, octylglucoside
BMDB, 1,4-bismaleimidyl-2,3-dihydroxybutane
BS^3, bis-sulfosuccinimidyl suberate
NEM, N-ethylmaleimide
PVDF, polyvinylidene difluoride
TBST, Tris-buffered saline-Tween 20

ACKNOWLEDGMENTS

REFERENCES

Applebury ML, Antoch MP, Baxter LC, et al. The murine cone photoreceptor: a single cone type expresses both S and M opsins with retinal spatial patterning. Neuron 2000;27:513–523. [PubMed: 11055434]

Balasubramanian S, Lynch JW, Barry PH. Calcium-dependent modulation of the agonist affinity of the mammalian olfactory cyclic nucleotide-gated channel by calmodulin and a novel endogenous factor. J Membr Biol 1996;152:13–23. [PubMed: 8660407]

Bauer PJ. Binding of the retinal rod Na+/Ca2+-K+ exchanger to the cGMP-gated channel indicates local Ca(2+)-signaling in vertebrate photoreceptors. Ann N Y Acad Sci 2002;976:325–334. [PubMed: 12502575]

Bauer PJ, Drechsler M. Association of cyclic GMP-gated channels and Na(+)-Ca(2+)-K+ exchangers in bovine retinal rod outer segment plasma membranes. J Physiol 1992;451:109–131. [PubMed: 1328615]

Bauer PJ, Schauf H. Mutual inhibition of the dimerized Na/Ca-K exchanger in rod photoreceptors. Biochim Biophys Acta 2002;1559:121–134. [PubMed: 11853679]

Biel M, Seeliger M, Pfeifer A, et al. Selective loss of cone function in mice lacking the cyclic nucleotide-gated channel CNG3. Proc Natl Acad Sci U S A 1999;96:7553–7557. [PubMed: 10377453]

Biel M, Zong X, Distler M, Bosse E, Klugbauer N, Murakami M, Flockerzi V, Hofmann F. Another member of the cyclic nucleotide-gated channel family, expressed in testis, kidney, and heart. Proc Natl Acad Sci U S A 1994;91:3505–3509. [PubMed: 8170936]

Bonigk W, Altenhofen W, Muller F, Dose A, Illing M, Molday RS, Kaupp UB. Rod and cone photoreceptor cells express distinct genes for cGMP-gated channels. Neuron 1993;10:865–877. [PubMed: 7684234]

Bonigk W, Muller F, Middendorff R, Weyand I, Kaupp UB. Two alternatively spliced forms of the cGMP-gated channel alpha-subunit from cone photoreceptor are expressed in the chick pineal organ. J Neurosci 1996;16:7458–7468. [PubMed: 8922401]

Brady JD, Rich ED, Martens JR, Karpen JW, Varnum MD, Brown RL. Interplay between PIP3 and calmodulin regulation of olfactory cyclic nucleotide-gated channels. Proc Natl Acad Sci U S A 2006;103:15635–15640. [PubMed: 17032767]

Bright SR, Rich ED, Varnum MD. Regulation of human cone cyclic nucleotide-gated channels by endogenous phospholipids and exogenously applied phosphatidylinositol 3,4,5-trisphosphate. Mol Pharmacol 2007;71:176–183. [PubMed: 17018579]

Chae KS, Ko GY, Dryer SE. Tyrosine phosphorylation of cGMP-gated ion channels is under circadian control in chick retina photoreceptors. Invest Ophthalmol Vis Sci 2007;48:901–906. [PubMed: 17251493]

Dang L, Pulukuri S, Mears AJ, Swaroop A, Reese BE, Sitaramayya A. Connexin 36 in photoreceptor cells: studies on transgenic rod-less and cone-less mouse retinas. Mol Vis 2004;10:323–327. [PubMed: 15152186]

Daniele LL, Lillo C, Lyubarsky AL, Nikonov SS, Philp N, Mears AJ, Swaroop A, Williams DS, Pugh EN Jr. Cone-like morphological, molecular, and electrophysiological features of the photoreceptors of the Nrl knockout mouse. Invest Ophthalmol Vis Sci 2005;46:2156–2167. [PubMed: 15914637]

Ding XQ, Fitzgerald JB, Matveev AV, McClellan ME, Elliott MH. Functional activity of photoreceptor cyclic nucleotide-gated channels is dependent on the integrity of cholesterol-and sphingolipid-enriched membrane domains. Biochemistry 2008;47:3677–3687. [PubMed: 18303857]

Ding XQ, Nour M, Ritter LM, Goldberg AF, Fliesler SJ, Naash MI. The R172W mutation in peripherin/rds causes a cone-rod dystrophy in transgenic mice. Hum Mol Genet 2004;13:2075–2087. [PubMed: 15254014]

Faillace MP, Bernabeu RO, Korenbrot JI. Cellular processing of cone photoreceptor cyclic GMP-gated ion channels: a role for the S4 structural motif. J Biol Chem 2004;279:22643–22653. [PubMed: 15024024]

Farjo R, Skaggs JS, Nagel BA, Quiambao AB, Nash ZA, Fliesler SJ, Naash MI. Retention of function without normal disc morphogenesis occurs in cone but not rod photoreceptors. J Cell Biol 2006;173:59–68. [PubMed: 16585269]

Gerstner A, Zong X, Hofmann F, Biel M. Molecular cloning and functional characterization of a new modulatory cyclic nucleotide-gated channel subunit from mouse retina. J Neurosci 2000;20:1324–1332. [PubMed: 10662822]

Gordon SE, Varnum MD, Zagotta WN. Direct interaction between amino-and carboxyl-terminal domains of cyclic nucleotide-gated channels. Neuron 1997;19:431–441. [PubMed: 9292731]

Grunwald ME, Zhong H, Lai J, Yau KW. Molecular determinants of the modulation of cyclic nucleotide-activated channels by calmodulin. Proc Natl Acad Sci U S A 1999;96:13444–13449. [PubMed: 10557340]

Hackos DH, Korenbrot JI. Calcium modulation of ligand affinity in the cyclic GMP-gated ion channels of cone photoreceptors. J Gen Physiol 1997;110:515–528. [PubMed: 9348324]

Haynes LW, Stotz SC. Modulation of rod, but not cone, cGMP-gated photoreceptor channels by calcium-calmodulin. Vis Neurosci 1997;14:233–239. [PubMed: 9147476]

Hirano AA, Hack I, Wassle H, Duvoisin RM. Cloning and immunocytochemical localization of a cyclic nucleotide-gated channel alpha-subunit to all cone photoreceptors in the mouse retina. J Comp Neurol 2000;421:80–94. [PubMed: 10813773]

Huttl S, Michalakis S, Seeliger M, et al. Impaired channel targeting and retinal degeneration in mice lacking the cyclic nucleotide-gated channel subunit CNGB1. J Neurosci 2005;25:130–138. [PubMed: 15634774]

Kang K, Bauer PJ, Kinjo TG, Szerencsei RT, Bonigk W, Winkfein RJ, Schnetkamp PP. Assembly of retinal rod or cone Na(+)/Ca(2+)-K(+) exchanger oligomers with cGMP-gated channel subunits as probed with heterologously expressed cDNAs. Biochemistry 2003;42:4593–4600. [PubMed: 12693957]

Kaupp UB, Niidome T, Tanabe T, et al. Primary structure and functional expression from complementary DNA of the rod photoreceptor cyclic GMP-gated channel. Nature 1989;342:762–766. [PubMed: 2481236]

Kaupp UB, Seifert R. Cyclic nucleotide-gated ion channels. Physiol Rev 2002;82:769–824. [PubMed: 12087135]

Kim TS, Reid DM, Molday RS. Structure-function relationships and localization of the Na/Ca-K exchanger in rod photoreceptors. J Biol Chem 1998;273:16561–16567. [PubMed: 9632727]

Kohl S, Baumann B, Broghammer M, et al. Mutations in the CNGB3 gene encoding the beta-subunit of the cone photoreceptor cGMP-gated channel are responsible for achromatopsia (ACHM3) linked to chromosome 8q21. Hum Mol Genet 2000;9:2107–2116. [PubMed: 10958649]

Kohl S, Marx T, Giddings I, Jagle H, Jacobson SG, Apfelstedt-Sylla E, Zrenner E, Sharpe LT, Wissinger B. Total colourblindness is caused by mutations in the gene encoding the alpha-subunit of the cone photoreceptor cGMP-gated cation channel. Nat Genet 1998;19:257–259. [PubMed: 9662398]

Li XF, Kiedrowski L, Tremblay F, et al. Importance of K+-dependent Na+/Ca2+-exchanger 2, NCKX2, in motor learning and memory. J Biol Chem 2006;281:6273–6282. [PubMed: 16407245]

Liu C, Varnum MD. Functional consequences of progressive cone dystrophy-associated mutations in the human cone photoreceptor cyclic nucleotide-gated channel CNGA3 subunit. Am J Physiol Cell Physiol 2005;289:C187–C198. [PubMed: 15743887]

Matulef K, Zagotta W. Multimerization of the ligand binding domains of cyclic nucleotide-gated channels. Neuron 2002;36:93–103. [PubMed: 12367509]

Mears AJ, Kondo M, Swain PK, Takada Y, Bush RA, Saunders TL, Sieving PA, Swaroop A. Nrl is required for rod photoreceptor development. Nat Genet 2001;29:447–452. [PubMed: 11694879]

Meyer MR, Angele A, Kremmer E, Kaupp UB, Muller F. A cGMP-signaling pathway in a subset of olfactory sensory neurons. Proc Natl Acad Sci U S A 2000;97:10595–10600. [PubMed: 10984544]

Misaka T, Kusakabe Y, Emori Y, Gonoi T, Arai S, Abe K. Taste buds have a cyclic nucleotide-activated channel, CNGgust. J Biol Chem 1997;272:22623–22629. [PubMed: 9278419]

Molday RS, Molday LL. Purification, characterization, and reconstitution of cyclic nucleotide-gated channels. Methods Enzymol 1999;294:246–260. [PubMed: 9916231]

Molokanova E, Savchenko A, Kramer RH. Interactions of cyclic nucleotide-gated channel subunits and protein tyrosine kinase probed with genistein. J Gen Physiol 2000;115:685–696. [PubMed: 10828243]

Muller F, Vantler M, Weitz D, Eismann E, Zoche M, Koch KW, Kaupp UB. Ligand sensitivity of the 2 subunit from the bovine cone cGMP-gated channel is modulated by protein kinase C but not by calmodulin. J Physiol 2001;532:399–409. [PubMed: 11306659]

Nikonov SS, Daniele LL, Zhu X, Craft CM, Swaroop A, Pugh EN Jr. Photoreceptors of Nrl −/− mice coexpress functional S-and M-cone opsins having distinct inactivation mechanisms. J Gen Physiol 2005;125:287–304. [PubMed: 15738050]

Nishiguchi KM, Sandberg MA, Gorji N, Berson EL, Dryja TP. Cone cGMP-gated channel mutations and clinical findings in patients with achromatopsia, macular degeneration, and other hereditary cone diseases. Hum Mutat 2005;25:248–258. [PubMed: 15712225]

Okada A, Ueyama H, Toyoda F, et al. Functional role of hCngb3 in regulation of human cone cng channel: effect of rod monochromacy-associated mutations in hCNGB3 on channel function. Invest Ophthalmol Vis Sci 2004;45:2324–2332. [PubMed: 15223812]

Paillart C, Winkfein RJ, Schnetkamp PP, Korenbrot JI. Functional characterization and molecular cloning of the K+-dependent Na+/Ca2+ exchanger in intact retinal cone photoreceptors. J Gen Physiol 2007;129:1–16. [PubMed: 17158950]

Paillart C, Zhang K, Rebrik TI, Baehr W, Korenbrot JI. Cloning and molecular characterization of cGMP-gated ion channels from rod and cone photoreceptors of striped bass (M. saxatilis) retina. Vis Neurosci 2006;23:99–113. [PubMed: 16597354]

Patel KA, Bartoli KM, Fandino RA, Ngatchou AN, Woch G, Carey J, Tanaka JC. Transmembrane S1 mutations in CNGA3 from achromatopsia 2 patients cause loss of function and impaired cellular trafficking of the cone CNG channel. Invest Ophthalmol Vis Sci 2005;46:2282–2290. [PubMed: 15980212]

Peng C, Rich ED, Thor CA, Varnum MD. Functionally important calmodulin-binding sites in both NH2- and COOH-terminal regions of the cone photoreceptor cyclic nucleotide-gated channel CNGB3 subunit. J Biol Chem 2003;278:24617–24623. [PubMed: 12730238]

Peng C, Rich ED, Varnum MD. Subunit configuration of heteromeric cone cyclic nucleotide-gated channels. Neuron 2004;42:401–410. [PubMed: 15134637]

Picones A, Korenbrot JI. Permeation and interaction of monovalent cations with the cGMP-gated channel of cone photoreceptors. J Gen Physiol 1992;100:647–673. [PubMed: 1334122]

Picones A, Korenbrot JI. Permeability and interaction of Ca2+ with cGMP-gated ion channels differ in retinal rod and cone photoreceptors. Biophys J 1995a;69:120–127. [PubMed: 7545443]

Picones A, Korenbrot JI. Spontaneous, ligand-independent activity of the cGMP-gated ion channels in cone photoreceptors of fish. J Physiol 1995b;485(Pt 3):699–714. [PubMed: 7562611]

Pugh, EN., Jr; a, LT. Handbook of Biological Physics. Elsevier/North-Holland: Amsterdam; 2000. Phototransduction in vertebrate rods and cones: molecular mechanisms of amplification, recovery and light adaptation.

Raven MA, Oh EC, Swaroop A, Reese BE. Afferent control of horizontal cell morphology revealed by genetic respecification of rods and cones. J Neurosci 2007;27:3540–3547. [PubMed: 17392470]

Rebrik TI, Korenbrot JI. In intact cone photoreceptors, a Ca2+-dependent, diffusible factor modulates the cGMP-gated ion channels differently than in rods. J Gen Physiol 1998;112:537–548. [PubMed: 9806963]

Rebrik TI, Korenbrot JI. In intact mammalian photoreceptors, Ca2+-dependent modulation of cGMP-gated ion channels is detectable in cones but not in rods. J Gen Physiol 2004;123:63–75. [PubMed: 14699078]

Rebrik TI, Kotelnikova EA, Korenbrot JI. Time course and Ca(2+) dependence of sensitivity modulation in cyclic GMP-gated currents of intact cone photoreceptors. J Gen Physiol 2000;116:521–534. [PubMed: 11004202]

Schwarzer A, Schauf H, Bauer PJ. Binding of the cGMP-gated channel to the Na/Ca-K exchanger in rod photoreceptors. J Biol Chem 2000;275:13448–13454. [PubMed: 10788457]

Shammat IM, Gordon SE. Stoichiometry and arrangement of subunits in rod cyclic nucleotide-gated channels. Neuron 1999;23:809–819. [PubMed: 10482246]

Sidjanin DJ, Lowe JK, McElwee JL, Milne BS, Phippen TM, Sargan DR, Aguirre GD, Acland GM, Ostrander EA. Canine CNGB3 mutations establish cone degeneration as orthologous to the human achromatopsia locus ACHM3. Hum Mol Genet 2002;11:1823–1833. [PubMed: 12140185]

Stricker HM, Ding XQ, Quiambao A, Fliesler SJ, Naash MI. The Cys214-->Ser mutation in peripherin/rds causes a loss-of-function phenotype in transgenic mice. Biochem J 2005;388:605–613. [PubMed: 15656787]

Sundin OH, Yang JM, Li Y, Zhu D, Hurd JN, Mitchell TN, Silva ED, Maumenee IH. Genetic basis of total colourblindness among the Pingelapese islanders. Nat Genet 2000;25:289–293. [PubMed: 10888875]

Trudeau MC, Zagotta WN. Mechanism of calcium/calmodulin inhibition of rod cyclic nucleotide-gated channels. Proc Natl Acad Sci U S A 2002;99:8424–8429. [PubMed: 12048242]

Trudeau MC, Zagotta WN. Calcium/calmodulin modulation of olfactory and rod cyclic nucleotide-gated ion channels. J Biol Chem 2003;278:18705–18708. [PubMed: 12626507]

Tsoi M, Rhee KH, Bungard D, Li XF, Lee SL, Auer RN, Lytton J. Molecular cloning of a novel potassium-dependent sodium-calcium exchanger from rat brain. J Biol Chem 1998;273:4155–4162. [PubMed: 9461611]

Varnum MD, Zagotta WN. Interdomain interactions underlying activation of cyclic nucleotide-gated channels. Science 1997;278:110–113. [PubMed: 9311913]

Weitz D, Ficek N, Kremmer E, Bauer PJ, Kaupp UB. Subunit stoichiometry of the CNG channel of rod photoreceptors. Neuron 2002;36:881–889. [PubMed: 12467591]

Weitz D, Zoche M, Muller F, Beyermann M, Korschen HG, Kaupp UB, Koch KW. Calmodulin controls the rod photoreceptor CNG channel through an unconventional binding site in the N-terminus of the beta-subunit. Embo J 1998;17:2273–2284. [PubMed: 9545240]

Wenzel A, von Lintig J, Oberhauser V, Tanimoto N, Grimm C, Seeliger MW. RPE65 is essential for the function of cone photoreceptors in NRL-deficient mice. Invest Ophthalmol Vis Sci 2007;48:534–542. [PubMed: 17251447]

Weyand I, Godde M, Frings S, Weiner J, Muller F, Altenhofen W, Hatt H, Kaupp UB. Cloning and functional expression of a cyclic-nucleotide-gated channel from mammalian sperm. Nature 1994;368:859–863. [PubMed: 7512693]

Wissinger B, Gamer D, Jagle H, et al. CNGA3 mutations in hereditary cone photoreceptor disorders. Am J Hum Genet 2001;69:722–737. [PubMed: 11536077]

Wissinger B, Muller F, Weyand I, Schuffenhauer S, Thanos S, Kaupp UB, Zrenner E. Cloning, chromosomal localization and functional expression of the gene encoding the alpha-subunit of the cGMP-gated channel in human cone photoreceptors. Eur J Neurosci 1997;9:2512–2521. [PubMed: 9517456]

Yu J, He S, Friedman JS, Akimoto M, Ghosh D, Mears AJ, Hicks D, Swaroop A. Altered expression of genes of the Bmp/Smad and Wnt/calcium signaling pathways in the cone-only Nrl-/-mouse retina, revealed by gene profiling using custom cDNA microarrays. J Biol Chem 2004;279:42211–42220. [PubMed: 15292180]

Yu WP, Grunwald ME, Yau KW. Molecular cloning, functional expression and chromosomal localization of a human homolog of the cyclic nucleotide-gated ion channel of retinal cone photoreceptors. FEBS Lett 1996;393:211–215. [PubMed: 8814292]

Zheng J, Trudeau MC, Zagotta WN. Rod cyclic nucleotide-gated channels have a stoichiometry of three CNGA1 subunits and one CNGB1 subunit. Neuron 2002;36:891–896. [PubMed: 12467592]

Zhong H, Molday LL, Molday RS, Yau KW. The heteromeric cyclic nucleotide-gated channel adopts a 3A:1B stoichiometry. Nature 2002;420:193–198. [PubMed: 12432397]

Zhu X, Brown B, Li A, Mears AJ, Swaroop A, Craft CM. GRK1-dependent phosphorylation of S and M opsins and their binding to cone arrestin during cone phototransduction in the mouse retina. J Neurosci 2003;23:6152–6160. [PubMed: 12853434]
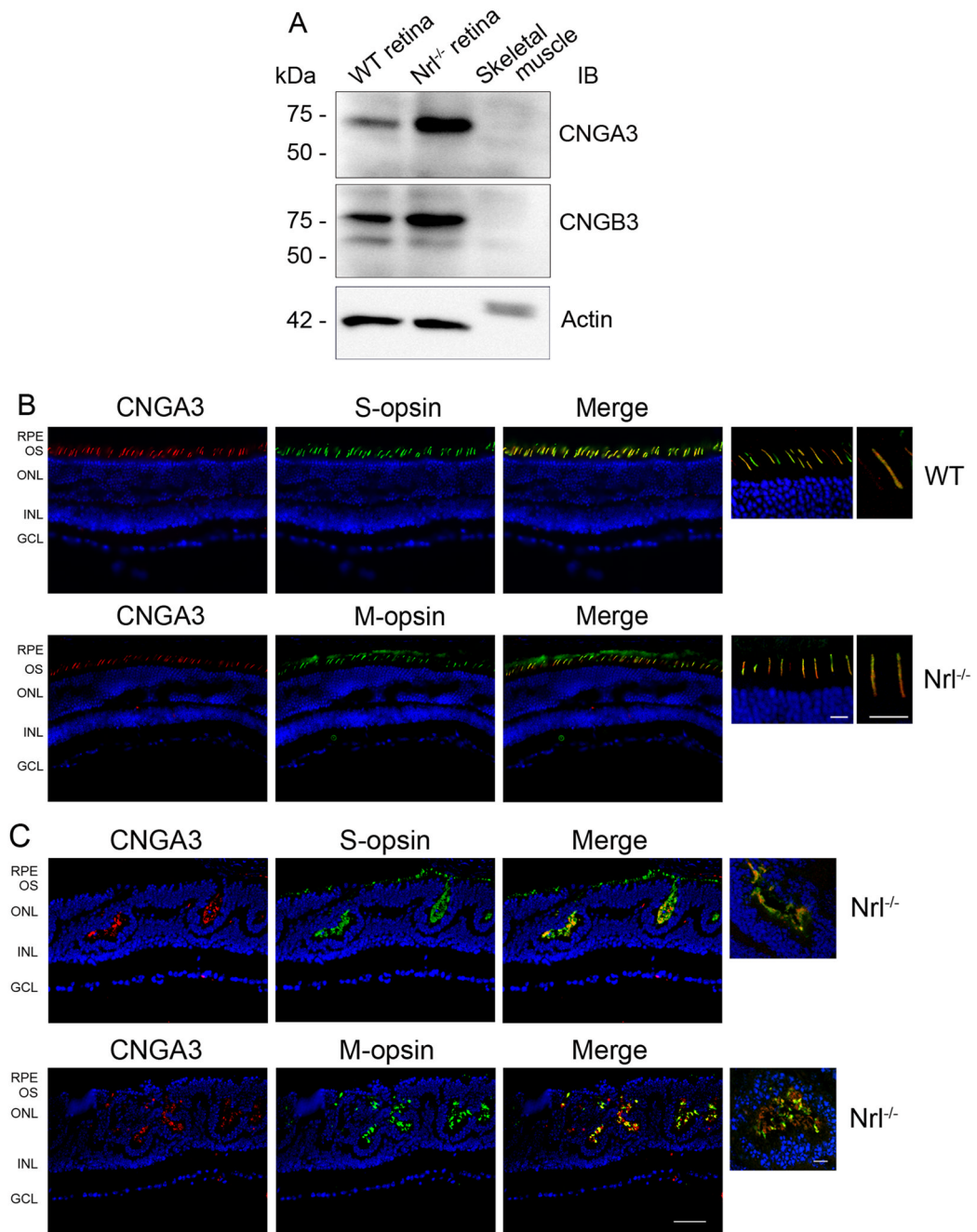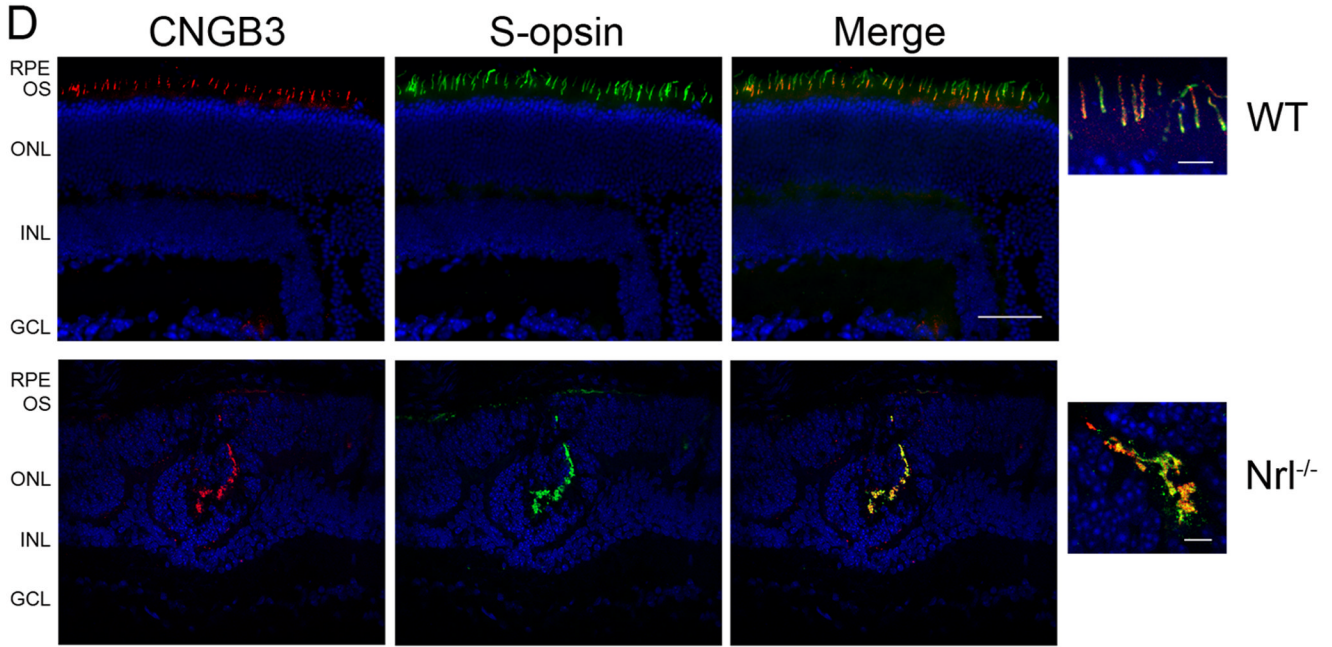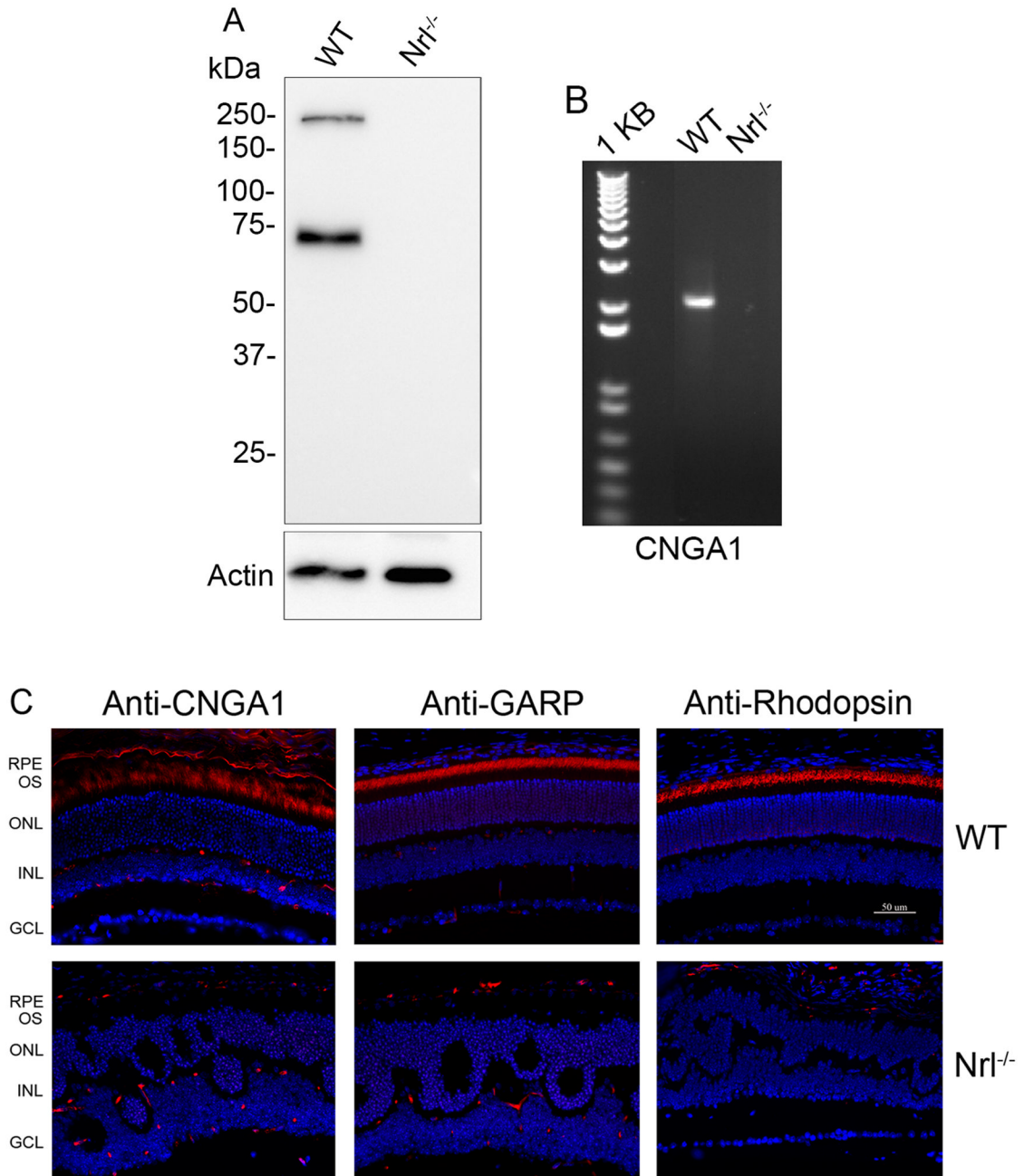
Figure 1.
Expression and cone localization of CNGA3 and CNGB3 in the mouse retina. *A*. Expression of CNGA3 and CNGB3 in the mouse retina detected by Western blotting. Retinal membranes prepared from wild-type and Nrl$^{-/-}$ mice were resolved by 10% SDS-PAGE, followed by immunoblotting using polyclonal anti-CNGA3 (upper panel) and anti-CNGB3 (middle panel) antibodies, respectively. Actin detection (lower panel) was included as a loading control. *B–D*. Cone localization of CNGA3 and CNGB3 detected by immunofluorescence labeling. Co-immunolabelings of CNGA3 with S-opsin or M-opsin in the wild-type (*B*) and Nrl$^{-/-}$ (*C*) retinal sections were performed using the rat monoclonal anti-CNGA3 (CNC-7D8) and the rabbit polyclonal anti-S-opsin or anti-M-opsin, respectively. Co-immunolabelings of CNGB3 with S-opsin in the wild type (*D*, upper panels) and Nrl$^{-/-}$ (*D*, lower panels) retinal sections were performed using the polyclonal anti-CNGB3 and the goat polyclonal anti-S-opsin. RPE, retinal pigment epithelium; OS, outer segment; ONL, outer nuclear layer; INL, inner nuclear layer; GCL, ganglion cell layer. Scale bar, 50 µm. Images of high magnification are shown to the right of the merge images for a better visualization of the co-localization. Scale bar, 10 µm.

Figure 2.
Lack of rod CNG channel expression in the Nrl$^{-/-}$ retina. *A*. Expression of CNGB1 in the wild-type but not in Nrl$^{-/-}$ retinas. Retinal membranes prepared from wild-type and Nrl$^{-/-}$ mice were resolved onto 10% SDS-PAGE and followed by Western blotting using the monoclonal anti-GARP (4B1). *B*. Expression of CNGA1 mRNA in the wild-type but not in Nrl$^{-/-}$ retinas analyzed by RT-PCR. Total RNA was prepared from wild-type and Nrl$^{-/-}$ retinas and cDNA were prepared and used in PCR using primers amplifying the full length of coding region of mouse CNGA1. *C*. Immunolabeling of CNGA1 (left panels) (using the monoclonal anti-CNGA1), GARP (middle panels) (using the monoclonal anti-GARP) and rhodopsin (right panels) (using the monoclonal anti-rhodopsin) in the wild-type but not in Nrl$^{-/-}$ retina. RPE,

retinal pigment epithelium; OS, outer segment; ONL, outer nuclear layer; INL, inner nuclear layer; GCL, ganglion cell layer. Scale bar, 50 µm.
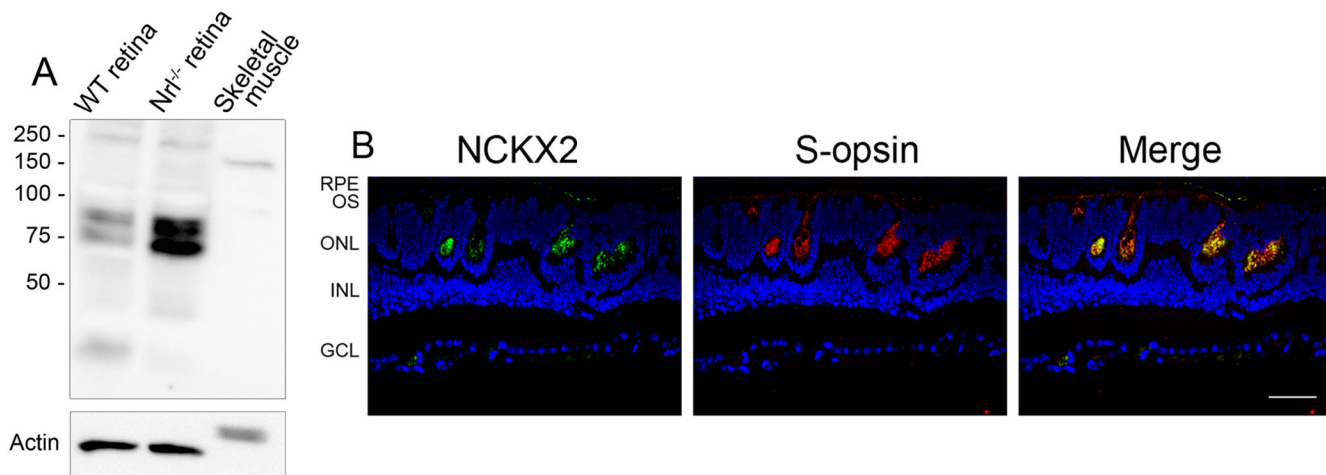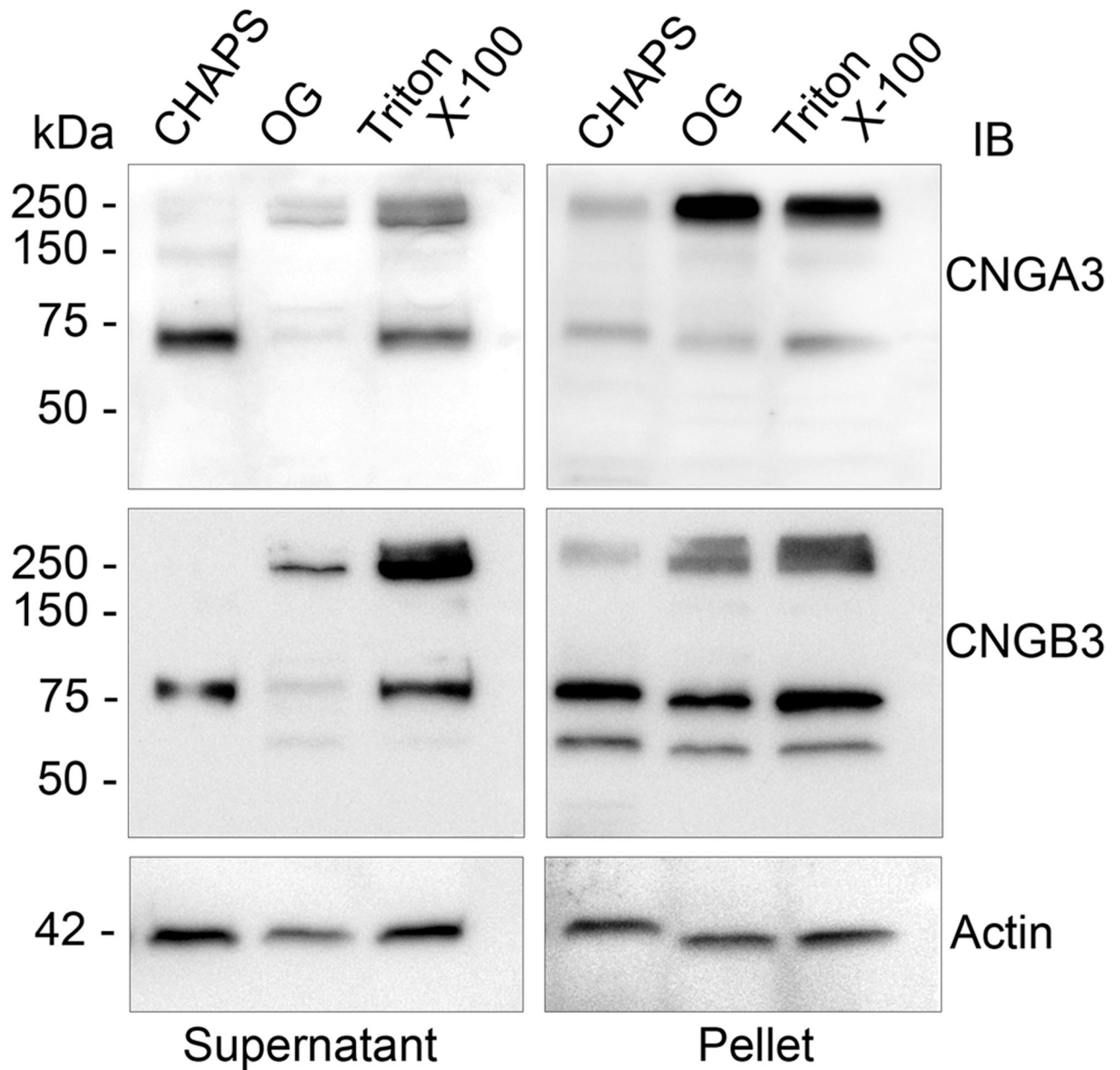
Figure 3.
Expression and cone localization of NCKX2 in the Nrl$^{-/-}$ retina. *A*. Expression of NCKX2 in the mouse retina detected by Western blotting. Retinal membranes prepared from wild-type and Nrl$^{-/-}$ mice were resolved by 10% SDS-PAGE and followed by immunoblotting using the polyclonal anti-NCKX2. *B*. Cone localization of NCKX2 in the Nrl$^{-/-}$ retina. Nrl$^{-/-}$ retinal sections were co-immunolabeled with the rabbit polyclonal anti-NCKX2 and the goat polyclonal anti-S-cone opsin. RPE, retinal pigment epithelium; OS, outer segment; ONL, outer nuclear layer; INL, inner nuclear layer; GCL, ganglion cell layer. Scale bar, 50 µm.

Matveev et al.

Page 22

Figure 4.
Detergent solubility of CNGA3 and CNGB3. Membrane preparations from Nrl$^{-/-}$ retinas were solubilized by Triton X-100, OG, and CHAPS and resulting supernatant and pellets were resolved by 10% SDS-PAGE, followed by Western blot analysis using the polyclonal anti-CNGA3 and polyclonal anti-CNGB3 antibodies, respectively. Actin detection was included as a loading control. Images shown are representative of three independent experiments.
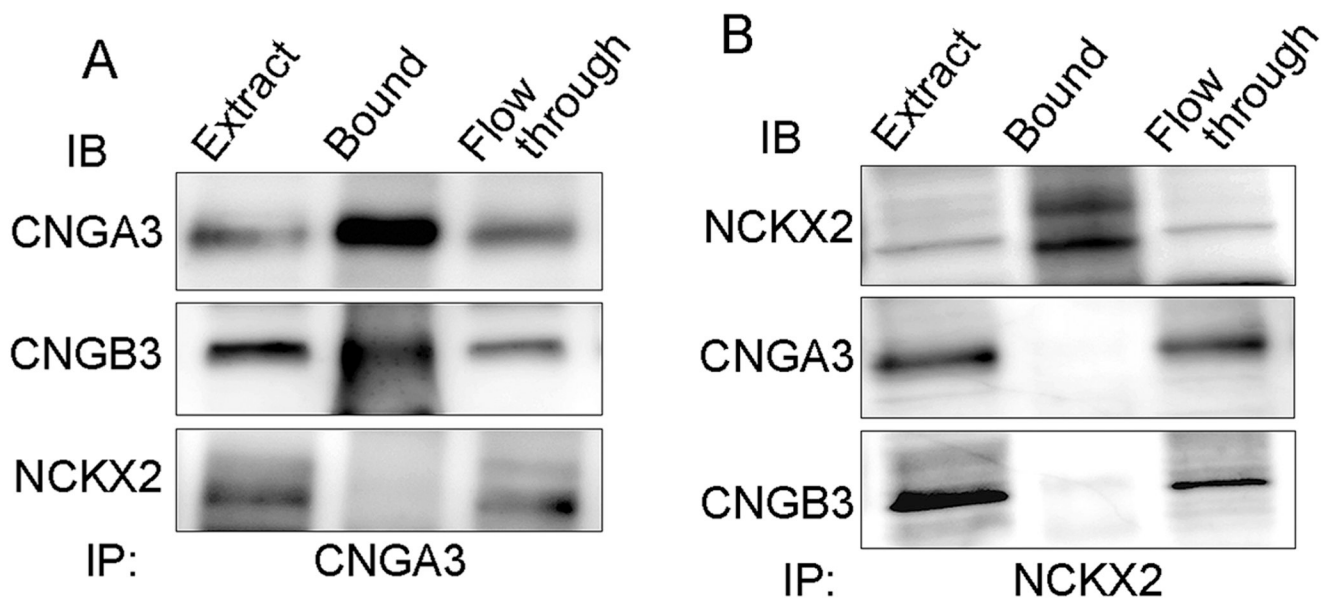
J Neurochem. Author manuscript; available in PMC 2009 October 2.

Figure 5.
Analysis of interactions of CNGA3 with CNGB3 and with NCKX2 in the mouse retina by co-immunoprecipitation. The CHAPS-solubilized membrane proteins prepared from Nrl$^{-/-}$ retinas were reacted with the polyclonal anti-CNGA3 (**A**) and the polyclonal anti-NCKX2 (**B**) antibodies in the immunoprecipitation assays. The resulting immunoprecipitants were resolved by 10% SDS-PAGE, followed by Western blotting using antibodies as indicated. Extract: solubilized membrane protein extracts used in immunoprecipitation assay. Images shown are representative of four independent experiments.
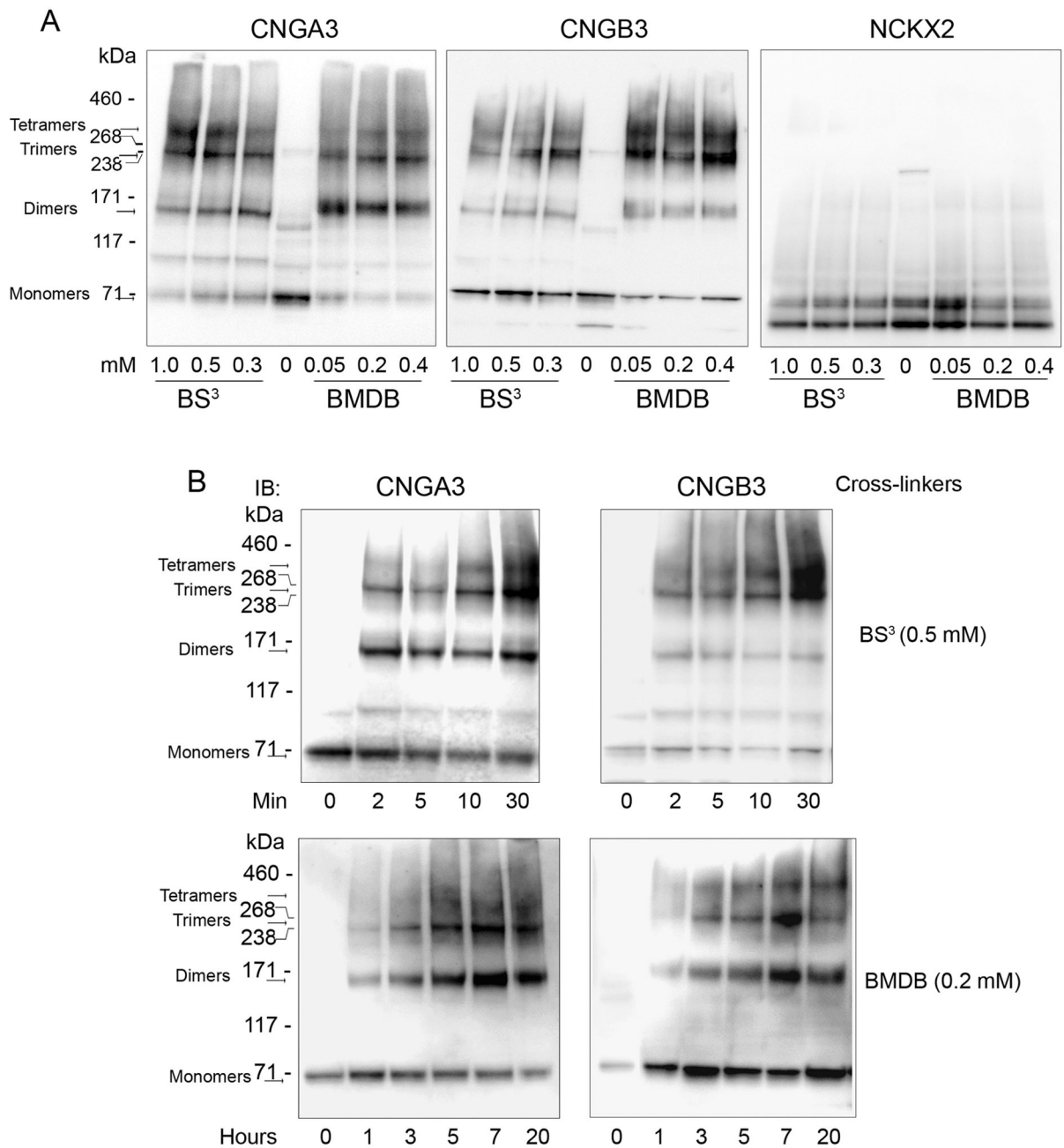
Figure 6.
Analysis of the mouse cone CNG channel complexes by chemical cross-linking. Retinal membranes prepared from Nrl$^{-/-}$ retinas were used in the chemical cross-linking reactions, using the thiol-specific cross-linker BMDB and the amino-specific cross-linker BS^3 at the varying concentrations (**A**) and durations (**B**) as indicated. The cross-linking products were separated by 3–8% Nu-PAGE, followed by immunoblotting using antibodies against CNGA3, CNGB3, and NCKX2, respectively. Images shown are representative of four independent experiments.
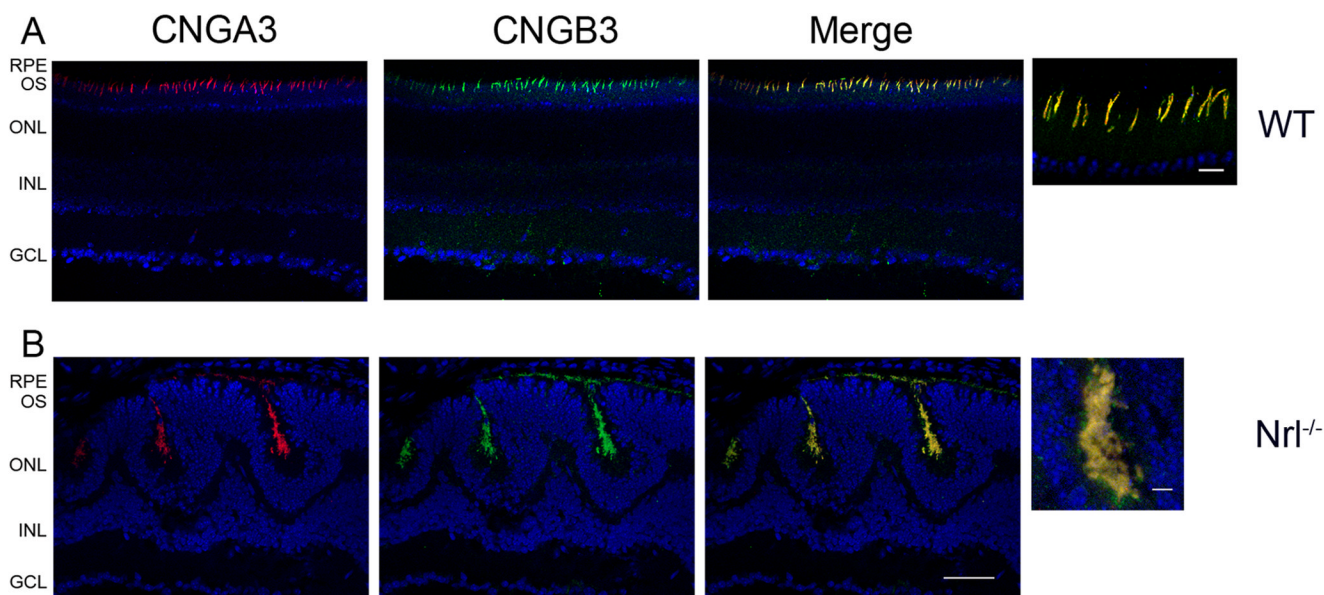
Figure 7.
Co-localization of CNGA3 and CNGB3 in the mouse retina. Cone localization of CNGA3 and CNGB3 in the wild-type (*A*) and Nrl$^{-/-}$ (*B*) retina. Co-immunolabeling of CNGA3 with CNGB3 in the wild-type and Nrl$^{-/-}$ retinal sections were performed using rat monoclonal anti-CNGA3 (CNC-7D8) and the rabbit polyclonal anti-CNGB3 antibodies. RPE, retinal pigment epithelium; OS, outer segment; ONL, outer nuclear layer; INL, inner nuclear layer; GCL, ganglion cell layer. Scale bar, 50 µm. Images of high magnification are shown to the right of the merge images for a better visualization of the co-localization. Scale bar, 10 µm.
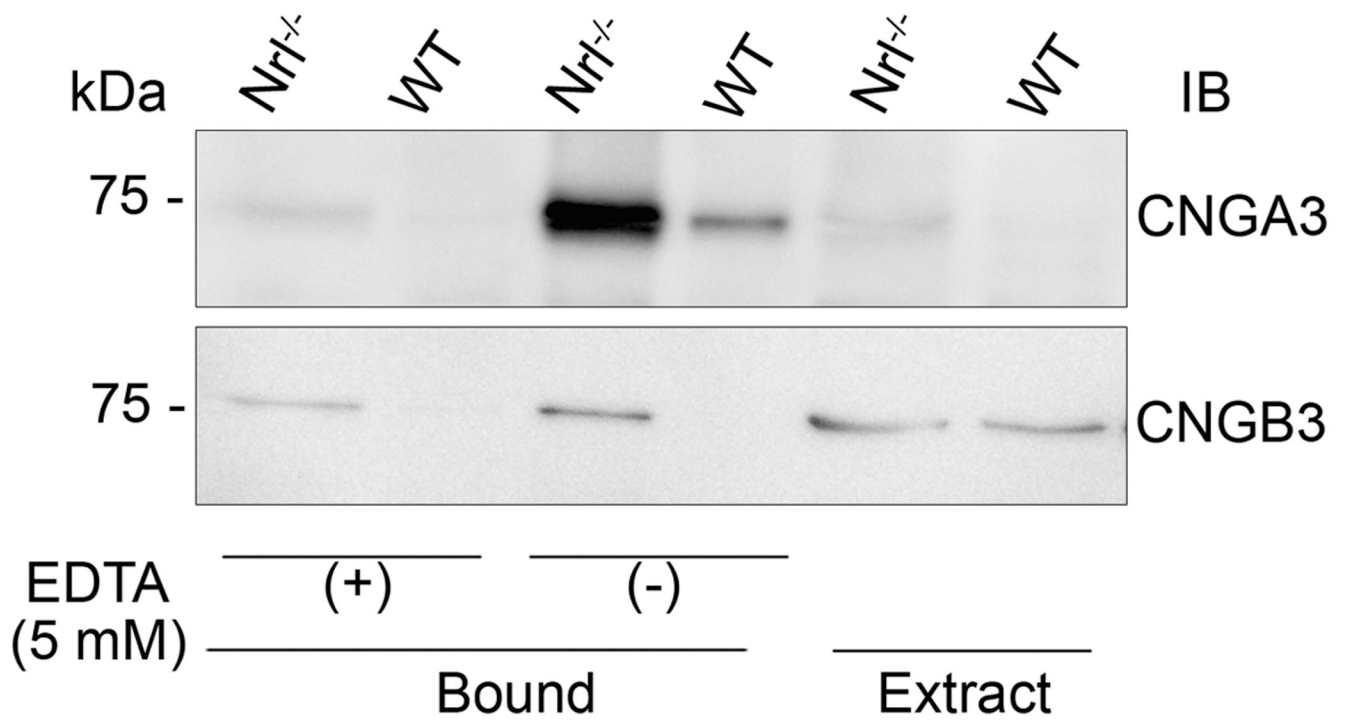
Figure 8.
Binding of CaM to cone CNG channel in the mouse retina. The CHAPS-solubilized membrane proteins prepared from mouse retinas were incubated with CaM resin in the CHAPS binding buffer in the presence or absence of 5 mM EDTA and bound proteins were eluted and resolved by 10% SDS-PAGE, followed by Western blotting. Extract: solubilized membrane protein extracts used in immunoprecipitation assay. Images shown are representative of three independent experiments.